CHARACTERIZATION AND CATALYTIC BEHAVIOR OF $MoO_3/V_2O_5/Nb_2O_5$ SYSTEMS IN ISOPROPANOL DECOMPOSITION

J. B. de Paiva Jr[1], W. R. Monteiro[2], M. A. Zacharias[2],
J. A. J. Rodrigues[2] and G. G. Cortez[1*]

[1]Laboratório de Catálise II, Escola de Engenharia de Lorena, Universidade de São Paulo,
Phone: +(55) (12) 3159-5105, Fax: +(55) 3153-3224, Rod. Itajubá-Lorena Km 74,5,
Campus I, CEP: 12600-000, Lorena, SP - Brasil.
E-mail: cortez@dequi.faenquil.br
[2]Laboratório Associado de Combustão e Propulsão, Instituto Nacional de Pesquisas Espaciais,
Phone: +(55) (12) 3186-9259, Fax: +(55) 3101-1992, Rod. Presidente Dutra Km 40,
CEP 12630-000, Cachoeira Paulista, SP - Brasil.
E-mail: jajr@lcp.inpe.br

Abstract - The influence of molybdenum oxide as a promoter on the V_2O_5/Nb_2O_5 system was investigated. A series of $MoO_3/V_2O_5/Nb_2O_5$ catalysts, with MoO_3 loading ranging from 1 to 3 wt% MoO_3 and fixed V_2O_5 content (21 wt%), were prepared by impregnation of the Nb_2O_5 support with an aqueous solution of ammonium metavanadate and ammonium molybdate. The acid-base properties of the catalysts were investigated to determine of the selectivity of the isopropanol decomposition reaction. The X-ray diffraction results showed the presence of the β-$(Nb,V)_2O_5$ phase. The temperature-programmed reduction profiles showed that the reducibility of vanadium was affected by the presence of molybdenum oxide. Activity results for isopropanol decomposition revealed that the acid-base properties of V_2O_5/Nb_2O_5 catalysts are affected upon incorporation of MoO_3, specifically for loadings of 3 wt %. For this catalyst composition both propylene and acetone formation rates decreased.
Keywords: Niobium oxide; Vanadium oxide; Molybdenum oxide; Isopropanol conversion.

INTRODUCTION

Supported vanadium oxide catalysts have been used in a great number of selective oxidation reactions (Cortez et al., 2003). The catalytic properties of the vanadium oxide are influenced strongly by several variables, such as method of preparation, nature of the support and promoter type. Vanadium and molybdenum oxides are important components of catalysts used for selective oxidation of light alkanes (Lopez Nieto et al., 1995). Molybdenum oxide has been used frequently as a promoter in V_2O_5-supported catalysts (Satsuma et al., 1991). Dejoz et al. (1999) reported the role of molybdenum in Mo-doped V-Mg-O catalysts during oxidative dehydrogenation of n-butane. Similarly, Lietti et al. (1999) showed that V_2O_5-MoO_3/TiO_2 catalysts could be used in the selective catalytic reduction (SCR) of NO_X In recent years niobium oxide-based systems have been employed as supports in numerous catalytic applications. The use of Nb_2O_5 as support in catalysts that contain vanadium can be a synergic alternative, since the two elements besides belonging to the same group in the periodic table, have several similar chemical properties (Tanabe, 2003). Catalytic applications of niobium oxide as support, promoter or a solid with acid properties have been reported in the last several years (Ziolek, 2003).

---

*To whom correspondence should be addressed

Isopropanol decomposition in the absence of oxygen is widely used as a chemical probe reaction to determine the acid-base properties of the catalysts. In the absence of oxygen the selectivity in the conversion of isopropanol into propylene by dehydration and acetone by dehydrogenation has been employed to determine the balance between surface acidity and basicity (Haffad et al., 2001). In the presence of oxygen, its reactivity is a measure of the surface redox potential of the catalyst or of its activity as a selective oxidation catalyst (Kulkarni and Wachs, 2002). The oxidation and decomposition reactions of isopropanol are analogous, since the only role of oxygen is to prevent the reduction of the metal oxide surface.

In the present study $MoO_3/V_2O_5/Nb_2O_5$ catalysts containing a fixed amount of V_2O_5 (21 wt.%) and MoO_3 loadings of 1 and 3 wt.% were prepared and characterized. The catalytic activity in the isopropanol decomposition was evaluated by cofeeding isopropanol and oxygen simultaneously.

EXPERIMENTAL

Prior to impregnation, the Nb_2O_5 was prepared by calcination of hydrated niobium oxide (supplied by CBMM, Brazil HY-340) at 500°C for 6 h. Preparation of V_2O_5/Nb_2O_5 catalysts involved two steps. In the first step, the support was added to an aqueous solution of NH_4VO_3 (Merck) salt kept at 70°C. The theoretical amount of vanadium in solution was selected in order to achieve 21 wt.% V_2O_5 in the final catalyst. The mixture was maintained under stirring at 70°C and the excess water was removed in a rotary evaporator. Then the impregnate was dried at 110°C for 12 h and subsequently calcined at 450°C for 4 h. In the second step, MoO_3 (1 or 3 wt.%) was incorporated by impregnating the V_2O_5/Nb_2O_5 catalyst with an aqueous solution of $(NH_4)_6Mo_7O_{24}.4H_2O$ (Mallinckrodt) salt. Drying and calcination of the ternary $MoO_3/V_2O_5/Nb_2O_5$ catalysts were the same as above for the binary V_2O_5/Nb_2O_5 systems. Samples are labeled xMo/21V/Nb, where x is MoO_3 loading (1 and 3 wt.%).

The contents of molybdenum and vanadium were determined by means of atomic absorption spectroscopy (AAS) using a Perkin-Elmer Analyst instrument, after extraction of metals from the catalysts samples in HNO_3 and HF acids.

Specific surface areas were calculated by the BET method from the nitrogen adsorption isotherms, measured with a Quantachrome NOVA 1000 instrument at − 196°C on 150 mg of sample that had previously been degassed at 200 °C in a high-vacuum atmosphere for 2 h.

XDR diffraction patterns were obtained with a Seifert Isodebyeflex 1001 diffractometer operated at 40 kV and 30 mA by Ni-filtered CuKα radiation (λ = 0.15418 nm). The samples in powder form were analyzed without previous treatment after deposition on a quartz sample holder. Crystalline phases was identified using references from the ASTM files.

Temperature-programmed reduction (TPR) results were obtained in a Quantachrome Chembet-3000 apparatus loaded with 25 mg of catalyst. The samples were first treated in helium at a temperature of 150°C for 1 h. The samples were cooled to room temperature and flown through them an H_2/N_2 mixture was subsequently (H_2/N_2 molar ratio of 0.15 and a total flow of 40 cm^3/min) and the samples heated at a rate of 10°C/min to a final temperature of 900°C.

The catalytic test of decomposition of the isopropanol was carried out in a fixed-bed quartz tubular reactor (i.d. 10 mm, length 400 mm) operated at atmospheric pressure and temperature in the range of 170-290°C. The reactor was equipped with a coaxial thermocouple for catalytic bed temperature profiling. The isopropanol (99.7%, Merck) was injected into the reactor with the aid of a Thermo Separation Product Spectra P100 pump at a flow rate of 0.05 cm^3/min and was diluted in a mixture of He and O_2 (molar ratio of 3/1 at a flow rate of 74 cm^3/min). Reactants and reaction products were analyzed by on-line gas chromatography (Varian 3350) with a thermal conductivity detector (TCD). A Carbowax 20M on a Chromosorb W column was used for separation of the products. The catalyst mass was 100 mg, the particle size 0.5-0.85 mm and the contact-time 2.5 g.h/mol$_{Isop}$. The conversion was calculated from the reaction product on the basis of the carbon balance: the total molar amount of carbon in the effluent was assumed to be equal to the molar amount of carbon in the isopropanol fed into the reactor.

RESULTS AND DISCUSSION

The results of the chemical composition determined by atomic absorption spectroscopy (AAS), BET specific areas and pore volumes of the samples are presented in Table 1. These results demonstrate that the amounts of V_2O_5 and MoO_3 in the samples are close to the theoretical values. The presence of vanadium on the Nb_2O_5 reduces both BET specific area and pore volume, this effect being more pronounced when molybdenum is added on the V_2O_5/Nb_2O_5 catalyst. This effect is related to the blockage of the Nb_2O_5 pores for the high loadings of V_2O_5 (21 wt.%) and also of MoO_3 (1 and 3 wt.%).

**Table 1: Results on the chemical composition of V and Mo obtained by AAS,
BET specific areas (Sg$_{BET}$) and pore volume (Vp) of the samples.**

Samples	V₂O₅ (wt.%)	MoO₃ (wt.%)	Sg$_{BET}$ (m²·g⁻¹)	Vp (cm³·g⁻¹)
Nb₂O₅	0	0	112	0.08
21V/Nb	24.2	0	39	0.04
1Mo/21V/Nb	21.0	1.2	17	0.02
3Mo/21V/Nb	19.2	2.9	6	nd

nd: not determined

In Figure 1 the XRD patterns of bulk V_2O_5, bulk MoO_3 and Nb_2O_5 support and of the catalyst xMo/21V/Nb calcined at 500°C are presented. The XRD profile of bulk V_2O_5 is presented in Figure 1-a, where the most intense peaks appear at 2θ angles of 20.3° (100%), 26.1° (90%) and 30.95° (85%). In Figure 1-b the XRD profiles of Nb_2O_5 are shown, with the most intense peak at 2θ = 23.14° corresponding to the TT-phase or T-phase of Nb_2O_5. The X-ray diffractograms of the calcined V_2O_5/Nb_2O_5 sample (Figure 1-c) show the presence of a β-$(Nb,V)_2O_5$ phase, as evidenced by the peaks at 2θ angles of 23.67°, 24.97° and 26.19°. A more intense peak at 2θ = 22.33° and other less intense ones are characteristic of V_2O_5 dispersed on Nb_2O_5. The absence of peaks of the crystalline MoO_3 phase for samples containing 1 and 3 wt.% MoO_3 supported on V_2O_5/Nb_2O_5, also included in Figures 1-d and 1-e, respectively, indicates that molybdenum oxide is amorphous or remains in a highly dispersed state on the V_2O_5/Nb_2O_5 system. The XRD profile of bulk MoO_3 is displayed in Figure 1-f, where the most intense peaks appear at 2θ angles of 27.3° (100%), 23.3° (55%) and 25.7° (44%). In previous studies, Ko and Weissman (1990) reported that, when calcined at 500°C, the forms of the TT and T-phases of Nb_2O_5 have a similar XRD pattern. Other authors (Chary et al., 2002) identified the TT-phase and T-phase of crystalline Nb_2O_5 with different spacing intensities at d = 3.94Å (2θ = 22.6°) and d = 3.14Å (2θ = 28.42°). The intensity of the β-$(Nb,V)_2O_5$ phase, identified at 2θ = 23.6° and 25.0°, increases with the addition of molybdena (1 wt.% of MoO_3) to the V_2O_5/Nb_2O_5 catalysts and decreases with the increase in molybdenum loading from 2 to 4 wt.%. In this study, this behavior was confirmed in all the samples. Recently, Chary et al. (2002) identified the β-$(Nb,V)_2O_5$ phase at 2θ angles of 22.5° (100%) and 28.5° (90%) for samples containing 10 to 12 wt.% V_2O_5 supported on Nb_2O_5. Watling et al. (1996) also observed the presence of the β-$(Nb,V)_2O_5$ phase for concentration of vanadium around 7 mol-% in vanadia-niobia catalysts.
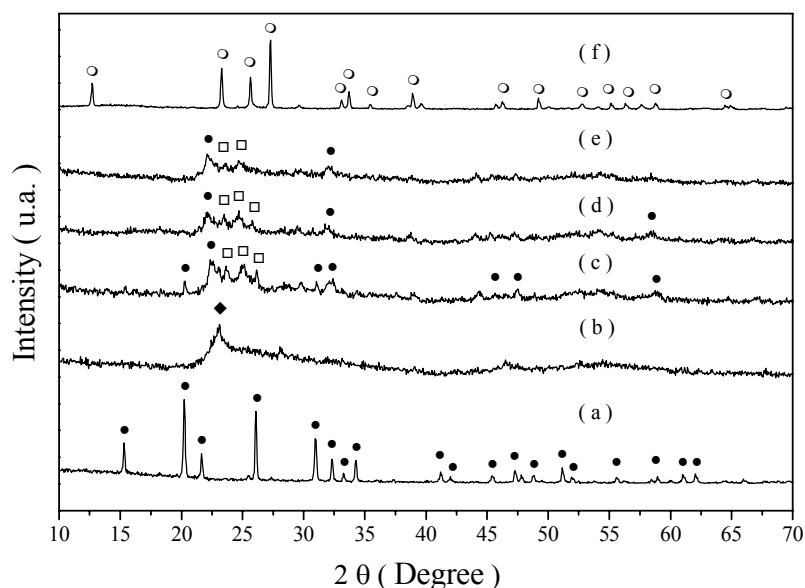
**Figure 1:** XDR patterns of (a) bulk V_2O_5; (b) N_2O_5; (c) 21V/Nb; (d) 1Mo/21V/Nb, (e) 3Mo/21V/Nb and (f) bulk MoO_3. Peaks due to (●) V_2O_5 phase; (◆) TT-phase or T-phase of Nb_2O_5, (□) β-$(Nb,V)_2O_5$ phase and (○) MoO_3 phase.

The temperature-programmed reduction (TPR) profiles of bulk V_2O_5, Nb_2O_5 and catalysts are presented in Figure 2. The TPR profile of pure V_2O_5 (in Figure 2-a) has three reduction peaks, at 663°C, 696°C and 836°C. Komandur et al. (2003) obtained the same profile, whose peaks were attributed to the following sequence of reduction of the vanadium oxide: 675°C ($V_2O_5 \rightarrow V_6O_{13}$), 705°C ($V_6O_{13} \rightarrow V_2O_4$) and 780°C ($V_2O_4 \rightarrow V_2O_3$). In the three reduction steps, vanadium (V^{+5}) is reduced to $V^{+4.33}$, V^{+4} and V^{+3} species whose ratios are an indication of the reduction temperature.

The reduction profile of Nb_2O_5, presented in Figure 2-b, shows a peak of reduction around 781°C. The reduction of Nb_2O_5 is more difficult than that of vanadium oxide. The complete reduction of pure niobium with hydrogen is initiated at 800°C.

However, the reduction of bulk Nb_2O_5 to Nb_2O_4 occurs at around 1300°C (Wachs et al., 2000). The 21V/Nb catalyst, shown in Figure 2-c, has four reduction peaks: a little defined one at around 595°C and the other three located at 640°C, 680°C and 830°C, the first three due to the reduction of the vanadium species and the last one corresponding to the reduction of Nb_2O_5. The reduction profile of 1Mo/21V/Nb catalyst, presented in Figure 2-d, shows four regions of reduction, at 608°C, 644°C, 692°C and 850°C. The presence of MoO_3 at low concentrations (1 wt.%) on V_2O_5/Nb_2O_5 modifies the reducibility of V^{+5} species, producting a significant change in the reduction temperatures for higher values. The reduction profile of 3Mo/21V/Nb catalyst (Figure 1-e) has two peaks with maximum at 630°C and 858°C.
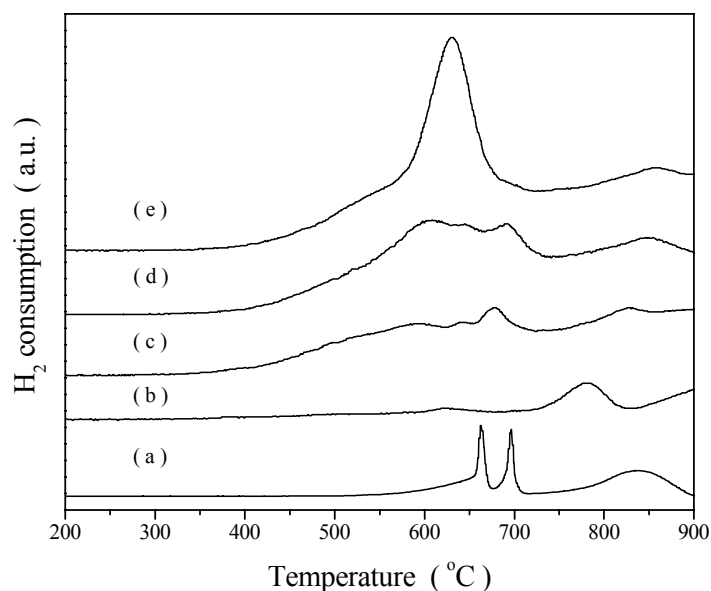
Figure 2: TPR profiles of (a) bulk V_2O_5; (b) Nb_2O_5; (c) 21V/Nb; (d) 1Mo/21V/Nb and (e) 3Mo/21V/Nb.

The modification of the reducibility of V^{+5} species in contact with the support can be attributed to the addition of molybdenum oxide through the formation of β-$(Nb,V)_2O_5$ phase, which produces an increase in the maximum temperature of reduction. Other authors (Chary et al., 2002) found that the addition of molybdenum oxide to V_2O_5/Nb_2O_5 catalysts favors the formation of β-$(Nb,V)_2O_5$ phase up to a loading of 3 wt.% MoO_3 and increases the reducibility of the catalysts. The reduction of MoO_3 was studied by Grunert et al. (1992). They identified several reduced species (Mo^{+6}, Mo^{+5}, Mo^{+4} and Mo^{+2}), together with another component located at around 630°C, which can be

attributed to the formation of metallic Mo. The TPR profile of unsupported MoO_3 is presented in Figure 3. The TPR profile of pure MoO_3 shows two major peaks, at 765 and 894°C. Recently, Bhaskar et al. (2001) identified two peaks of reduction of bulk MoO_3, at 767 and 997°C and a minor one at 797°C. The sharp peak at 767°C corresponds to the reduction of MoO_3 ($MoO_3 \rightarrow MoO_2$) and the peak at 997°C is associated with the reduction of MoO_2 ($MoO_2 \rightarrow Mo$). A minor peak at 797°C can correspond to Mo_4O_{11} formed by reduction of MoO_3. In the present work, a reduction peak at 630°C (Figure 2-e) can be attributed to the metallic Mo reduced on V_2O_5/Nb_2O_5.
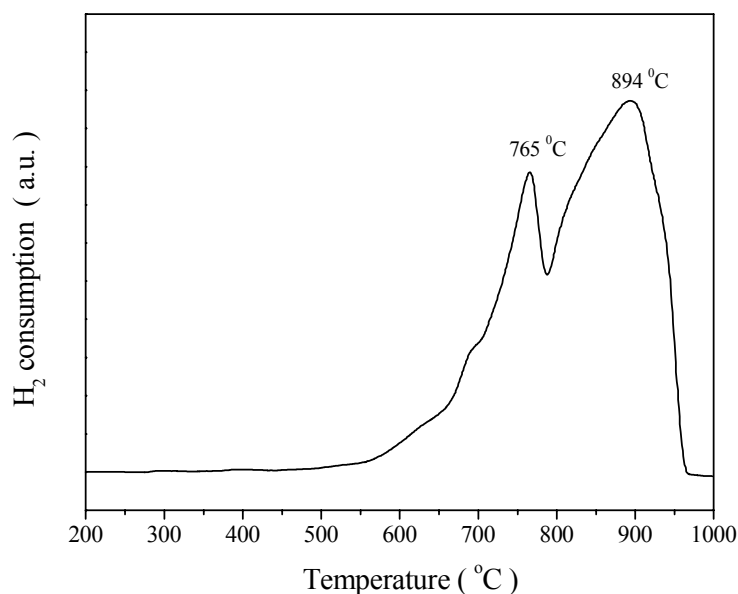
Figure 3: TPR profile of unsupported MoO_3.

The acid-base properties of catalysts were compared using the isopropanol test reaction. The results of catalytic activity for the oxidative decomposition of isopropanol as a function of reaction temperature are shown in Table 2.

The catalytic activity was evaluated considering the rate of formation of the products as base (mol $g_{cat}^{-1}min^{-1}$). The results show that the Nb_2O_5 is only selective to propylene at a temperature of 230°C. Incorporation of vanadium on niobium oxide produces propylene and acetone in the three temperature ranges, with intervals their ratio increasing from one temperature range to the next. The addition of 1 wt.% of MoO_3 to 21V/Nb catalyst increases propylene production and reduces the

production of acetone. The production of both propylene and acetone decreases in the 3Mo/21V/Nb catalyst.

The results of catalytic activity versus reaction temperature for isopropanol decomposition on 1Mo/21V/Nb catalyst are shown in Figure 4. Conversion of the isopropanol increases with the rise in temperature and reaches a maximum at a temperature of 260°C. Propylene formation is favored by starting at the temperature of 210°C; however the formation of acetone and di-isopropylether follows an opposite trend. This means, in agreement with previous observations (Wang et al., 1999), that an increase in temperature favors propylene formation through the dehydration route of isopropanol.

**Table 2: Results on the catalytic activity of Nb₂O₅ and xMo/21V/Nb
at different temperatures in isopropanol decomposition.**

Catalyst	RFP - Rate of formation of the products (10^{-4}mol $g_{cat}^{-1}min^{-1}$)					
	Propylene			Acetone		
	210°C	220°C	230°C	210°C	220°C	230°C
Nb_2O_5	0	0	8.1	0	0	0
21V/Nb	38.8	46.6	51.5	14.3	13.0	11.1
1Mo/21V/Nb	33.4	46.9	55.1	4.8	4.7	4.5
3Mo/21V/Nb	5.5	35.8	43.1	4.0	3.0	2.8
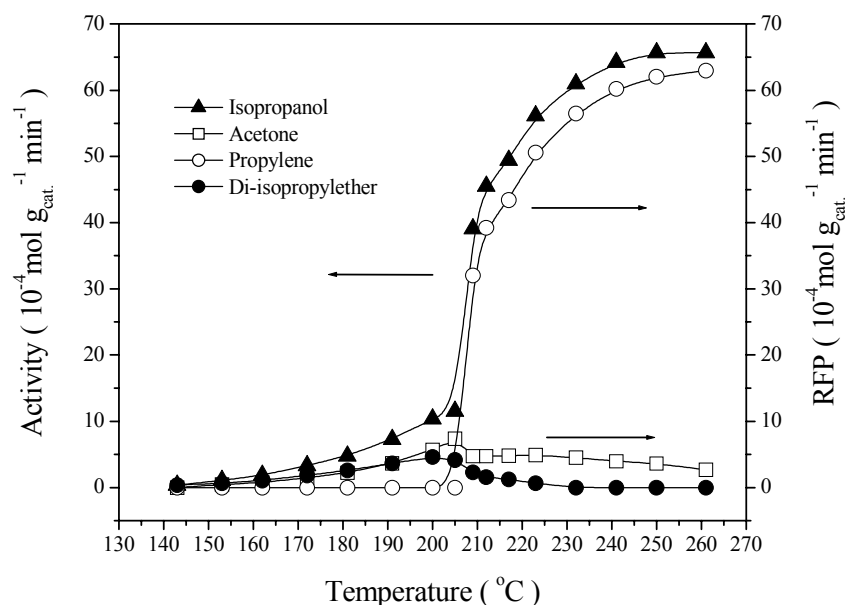
Figure 4: Results on catalytic activity versus reaction temperature for the isopropanol decomposition on 1Mo/21V/Nb catalyst. (▲) Isopropanol; (○) Propylene; (□) Acetone and (●) Di-isopropylether.

It is known that the decomposition of isopropanol can occur through different mechanisms, which depend on the acid and basic properties of the catalyst (Gervasini et al., 1997). The dehydration carried out on acid sites or concerted acid-base pair sites gives propylene and diisopropyl ether, and dehydrogenation gives acetone on basic sites. Ether formation must involve an inner-molecular coupling reaction. Identification of the acid and basic properties of the catalyst can determine the mechanism that is most probable in this reaction (Díez et al., 2003). On the other hand, the reaction of decomposition of isopropanol does not provide information to distinguish between the Lewis and Brönsted acids sites. The presence of redox species in the catalysts can contribute to dehydration and dehydrogenation in the decomposition of isopropanol. Deo and Wachs (1994) identified the surface species of vanadium oxide on different metal oxides. The VO_4 species on γ-Al_2O_3 are detected at low concentrations of vanadium oxide, and even polymeric species of the V-O-V type occur happen with an increase in concentration of vanadium oxide (Cortez et al., 2002). At higher concentrations, the formation of three-dimensional crystals of V_2O_5, in which vanadium is octahedrally coordinated by oxygen ions (Arena et al., 1999), is observed. In this work only a high vanadium concentration was used

on Nb_2O_5, for which XRD patterns revealed the appearance of crystalline phase V_2O_5.

The acid character of Nb_2O_5, V_2O_5 and MoO_3 oxides has been reported in the literature. Jehng and Wachs (1990) studied the molecular structure-reactivity relationships for supported niobium oxide catalysts by combining Raman spectroscopy structural studies with chemical probes (pyridine) that measured the acidity and reactivity of the surface niobium oxide sites. Raman spectroscopy showed that the highly distorted NbO_6 octahedron has Nb-O bonds that are associated with the Lewis acid sites with bands between 850 cm^{-1} and 1000 cm^{-1}. The slightly distorted NbO_6 octahedron as well as NbO_7 and NbO_8 groups has only Nb-O bonds and is associated with the Brönsted acid sites. Busca et al. (1989) found acidity of the Lewis and Brönsted types on V_2O_5. The formation of surface vanadia species on the oxide supports is accompanied by a decrease in the number of surface Lewis acid sites and increase in the number of surface Brönsted acid sites (Blasco et al., 1997). The decrease in Lewis acidity can be associated with the coordination of VO_X species on the support, and the increase in Brönsted acidity to the V-OH groups of the VOH_4^{-2} and $V_2O_7H_2^{-2}$ species on the support (Ferreira and Volpes, 1999). In studies on TPD of NH_3 adsorption on Mo/γ-Al_2O_3, some authors (Abello et al., 2001)

observed that the addition of Mo on γ-Al$_2$O$_3$ increases the number of acid sites that interact with NH$_3$. Accordingly, there is an important decrease in acid strength with an increase in molybdenum oxide loading, and new acid sites of weak and moderate strength are formed. In previous work, Aramendía et al. (1996) concluded that the activity of dehydration in the reaction of decomposition of isopropanol on MgO is related to Brönsted acidity. Similar results were found by Martin et al. (1996) for MoO$_3$/TiO$_2$ catalysts.

The results of the present paper confirm that propylene formation on *x*Mo/21V/Nb catalysts is due to the presence of acid sites of weak and moderate strength (Brönsted acid sites) generated on the surface of the catalyst by V$_2$O$_5$ and MoO$_3$ oxides. The formation of acetone was due to the presence of basic sites related to the surface oxygen of VO$_X$ and MO$_X$ moieties on niobium oxide.

CONCLUSIONS

Incorporation of vanadium on the Nb$_2$O$_5$ support and of molybdenum on the V/Nb system resulted in a significant drop in specific area and pore volume of niobium oxide substrate, with this effect being more pronounced when the content of MoO$_3$ was 3 wt.%. By XRD, it was verified that the addition of vanadium to Nb$_2$O$_5$ results in the formation of the β-(Nb,V)$_2$O$_5$ phase, and the addition of molybdenum the V/Nb system distorts the intensity of the peaks of this crystalline phase. The addition of molybdenum at low concentrations modifies the reducibility of vanadium on Nb$_2$O$_5$, increasing the maximum temperature of reduction. The presence of 3 wt.% MoO$_3$ to the V/Nb system affects the reducibility of VO$_X$ species in the catalyst.

In the catalyst with a low MoO$_3$ content, the results of catalytic activity showed a high selectivity to propylene. This fact is related to the presence of Brönsted acid sites in the catalyst with a low concentration of MoO$_3$. This effect is due to the decrease in strong acid sites (Lewis) and the increase in acid sites of weak and moderate acid strength (Brönsted) upon addition of MoO$_3$.

ACKNOWLEDGMENTS

REFERENCES

Abello, M.C., Gomez, M.F. and Ferretti, O., Mo/γ-Al$_2$O$_3$ Catalysts for the Oxidative Dehydrogenation of Propane: Effect of Mo Loading, Applied Catal. A: Gen. 207, 421 (2001).

Aramendía, M.A., Borau, V., Jimenez, C., Marinas, J.M., Porras, A. and Urbano, F.J., Magnesium Oxides as Basic Catalysts for Organic Processes, J. Catal. 161, 829 (1996).

Arena, F., Frusteri, F., Parmaliana, A., Structure and Dispersion of Supported-vanadia Catalysts. Influence of the Oxide Carrier, Appl. Catal. A: Gen. 176, 189 (1999).

Bhaskar, T., Reddy, K.R., Kumar, C.P., Murthy, M.R.V.S. and Chary, K.V.R., Characterization and Reactivity of Molybdenum Oxide Catalysts Supported on Zirconia, Appl. Catal. A: Gen. 211, 189 (2001).

Blasco, T., Galli, A., López Nieto, J.M. and Trifiró, F., Oxidative Dehydrogenation of Ethane and n-Butane on VO$_x$/Al$_2$O$_3$ Catalysts, J. Catal. 169, 203 (1997).

Busca, G., Ramis, G. and Lorenzelli, V., FT-IR Study of the Surface Properties of Polycrystalline Vanadia, J. Mol. Catal. 50, 231 (1989).

Chary, K.V.P., Kumar, C.P., Peddy, K.R., Bhaskar, T. and Rajiah, T., Characterization and catalytic properties of MoO$_3$-V$_2$O$_5$/Nb$_2$O$_5$, Catal. Commun. 3, 7 (2002).

Cortez, G.G. and Bañares, M.A., A Raman Spectroscopy Study of Alumina-Supported Vanadium Oxide Catalyst during Propane Oxidative Dehydrogenation with Online Activity Measurement, J. Catal. 209, 197 (2002).

Cortez, G.G, Fierro, J.L.G. and Bañares, M.A., Role of Potassium on the Structure and Activity of Alumina-Supported Vanadium Oxide Catalysts for Propane Oxidative Dehydrogenation, Catal. Today 78, 219 (2003).

Datka, J., Turek, A.M., Jehng, J.M. and Wachs, I.E., Acidic Properties of Supported Niobium Oxide Catalysts: An Infrared Spectroscopy Investigation, J. Catal. 135, 186 (1992).

Dejoz, A., López Nieto, J.M., Márquez, F. and Vázquez, M.I., The Role of Molybdenum in Mo-doped V–Mg–O Catalysts During the Oxidative

Dehydrogenation of n-Butane, Appl. Catal. A: Gen. 180, 83 (1999).

Deo, G. and Wachs, I.E., Reactivity of Supported Vanadium Oxide Catalysts: The Partial Oxidation of Methanol, J. Catal. 146, 323 (1994).

Díez, V.K., Apestegía, C.R. and Di Cosimo, J.I., Effect of the Chemical Composition on the Catalytic Performance of Mg_yAO_x Catalysts for Alcohol Elimination Reactions, J. Catal. 215, 220 (2003).

Ferreira, M.L. and Volpe, M., On the Nature of Highly Dispersed Vanadium Oxide Catalysts: Effect of the Support on the Structure of VO_X Species, J. Mol. Catal. 149, 32 (1999).

Gervasini, A., Fenyvesi, J. and Auroux, A., Study of the Acidic Character of Modified Metal Oxide Surfaces Using the Test of Isopropanol Decomposition, Catal. Lett. 43, 219 (1997).

Gooding, W.B., Pekny, J.F. and McCroskey, P.S., Enumerative Approaches to Parallel Flowshop Scheduling via Problem Transformation, Comp. Chem. Engin. 18, 909 (1994).

Grünert, W., Stakheev, A.Y., Mörke, W., Feldhaus, R., Anders, K., Shapiro, E.S. and Minachev, K.M., Reduction and Metathesis Activity of MoO_3/Al_2O_3 Catalysts: I. An XPS Investigation of MoO_3/AI_2O_3, J. Catal. 135, 269 (1992).

Haffad, D., Chambellan, A. and Lavalley, J.C., Propan-2-ol Transformation on Simple Metal Oxides TiO_2, ZrO_2 and CeO_2, J. Mol. Catal. A: Chem. 168, 153 (2001).

Jehng, J.M. and Wachs, I.E., The Molecular Structures and Reactivity of Supported Niobium Oxide Catalysts, Catal. Today, 8, 37 (1990).

Ko, E.I. and Weissman, J.G., Structures of Niobium Pentoxide and their Implications on Chemical Behavior, Catal. Today 8, 27 (1990).

Komandur, V.R.C., Chinthala, P.K., Kondakindi, R.R., Thallada, B. and Taduri, R., Characterization and Catalytic Properties of MoO_3-V_2O_5/Nb_2O_5 Catalysts, Catal. Commun. 3, 7 (2002).

Komandur, V.R.C., Gurram, K., Chinthala, P.K., Guggilla, V.S. and Niemantsverdriet, J.W.,

Characterization and Reactivity of Vanadium Oxide Catalysts Supported on Niobia, Appl. Catal. A: Gen. 245, 303 (2003).

Kulkarni, D. and Wachs, I.E., Isopropanol Oxidation by Pure Metal Oxide Catalysts: Number of Active Surface Sites and Turnover Frequencies, Appl. Catal. A: Gen. 237, 121 (2002).

Lietti, L., Nova, I., Ramis, G., Dall'Acqua, L., Busca, G., Giamello, E., Forzatti, P. and Bregani, F., Characterization and Reactivity of V_2O_5-MoO_3/TiO_2 De-NOx SCR Catalysts, J. Catal. 187, 419 (1999).

Lopez Nieto, J.M., Dejoz, A. and Vazquez, M.I., Preparation, Characterization and Catalytic Properties of Vanadium Oxides Supported on Calcined Mg/Al-hydrotalcite, Appl. Catal. A: Gen. 132, 41 (1995).

Martin, C., Martin, I., Rives, V. and Malet, P., Alkaline-Metal Doped MoO_3/TiO_2 Systems: Structure of Supported Molybdates, J. Catal. 161, 87 (1996).

Satsuma, A., Okada, F., Hattori, A., Miyamoto, A., Hattori, T. and Murakami, Y., Promotion Effects of Various Oxides on Oxidation of Benzene Over Vanadium Pentoxide Catalysts, Appl. Catal. 72, 295 (1991).

Tanabe, K., Catalytic Application of Niobium Compounds, Catalysis Today, 78, 65 (2003).

Wachs, I.E., Briand, L.E., Jehng, J.M., Burcham, L. and Gao, X., Molecular Structure and Reactivity of the Group V Metal Oxides, Catal. Today 57, 323 (2000).

Wang, J.A., Bokhimi, X., Novaro, O., Lopez, T. and Gomez, R., Effects of the Surface Structure and Experimental Parameters on the Isopropanol Decomposition Catalyzed with Sol-gel, J. Mol. Catal. A: Gen. 145, No 1, 291 (1999).

Watling, T.C., Deo, G., Seshan, K., Wachs, I.E. and Lercher, J.A., Oxidative Dehydrogenation of Propane Over Niobia Supported Vanadium Oxide Catalysts, Catal. Today 28, 139 (1996).

Ziolek, M., Niobium-containing Catalysts - The State of the Art, Catal. Today 78, 47 (2003).